Available online at www.sciencedirect.com
ScienceDirect
Earth and Planetary Science Letters 259 (2007) 212–225
EPSL
www.elsevier.com/locate/epsl

Modeling the evolution of continental subduction processes in the Pamir–Hindu Kush region

Ana M. Negredo [a,*], Anne Replumaz [b], Antonio Villaseñor [c], Stéphane Guillot [d]

[a] Department of Geophysics, Facultad CC. Físicas, Universidad Complutense de Madrid. Av. Complutense, 28040 Madrid, Spain
[b] Université Lyon 1 and ENS-Lyon, LST, UMR CNRS 5570 Bât géode, 2 rue Dubois, 69622 Villeurbanne Cedex, France
[c] Instituto de CC. de la Tierra 'Jaume Almera', CSIC, C/Lluís Solé i Sabarís, s/n. 08028 Barcelona, Spain
[d] Université Joseph Fourier, LGCA, UMR CNRS 5025, 1381 rue de la Piscine. 38400 St Martin d'Heres Cedex, France

Received 13 November 2006; received in revised form 17 April 2007; accepted 30 April 2007
Available online 8 May 2007
Editor: C.P. Jaupart

Abstract

Several geological and geophysical studies suggest the presence of two converging subduction zones in the western syntaxis of the India–Eurasia collision zone, with steep northward subduction of Indian lithosphere beneath the Hindu Kush and southward subduction of Asian lithosphere under the Pamir. We investigate the geometry and the timing of these subduction processes. Seismic tomography images are used to constrain the geometry of the two slabs under the Pamir and the Hindu Kush. By measuring the tomographically inferred length of the Indian slab under the Hindu Kush region and by comparison with paleomagnetic reconstructions, we estimate that the process of Indian slab break-off most likely occurred at the early stage of the collision, at ca. 44–48 Ma. We infer that after slab break-off, western India continued its northward motion until its northern boundary reached the present Hindu Kush region, where it began to subduct. We estimate an age for the initiation of subduction in this region of about 8 Ma. We apply 2D thermo-kinematic and rheological numerical modeling to compute the temperature distribution and brittle field along two vertical sections across the Hindu Kush and Pamir regions. For the Hindu Kush we introduce parameters reproducing fast and near vertical subduction, whereas in the Pamir region we use the results from published studies to reproduce slower subduction. Modeling results indicate that faster subduction under the Hindu Kush results in a deeper brittle region, which is consistent with observed deeper seismicity than in the Pamir region.

Keywords: Hindu Kush; Pamir; continental subduction; numerical modeling; temperature; rheology

1. Introduction

The area of the Hindu Kush and Pamir seismic regions, located in the western syntaxis of the India–Eurasia collision zone (Fig. 1), is one of the most active areas of intermediate-depth seismicity in the world, and by far the most active area of intermediate-depth seismicity not clearly associated with oceanic subduction. The three-dimensional pattern of seismicity is characterized by the change in the dip of seismicity from steeply north dipping beneath the Hindu Kush to southward dipping under the Pamir (Fig. 1). A first model suggests that intermediate-depth seismicity is

* Corresponding author.
E-mail addresses: anegredo@fis.ucm.es (A.M. Negredo), anne.replumaz@univ-lyon1.fr (A. Replumaz), antonio@ija.csic.es (A. Villaseñor), sguillot@ujf-grenoble.fr (S. Guillot).

0012-821X/$ - see front matter © 2007 Published by Elsevier B.V.
doi:10.1016/j.epsl.2007.04.043

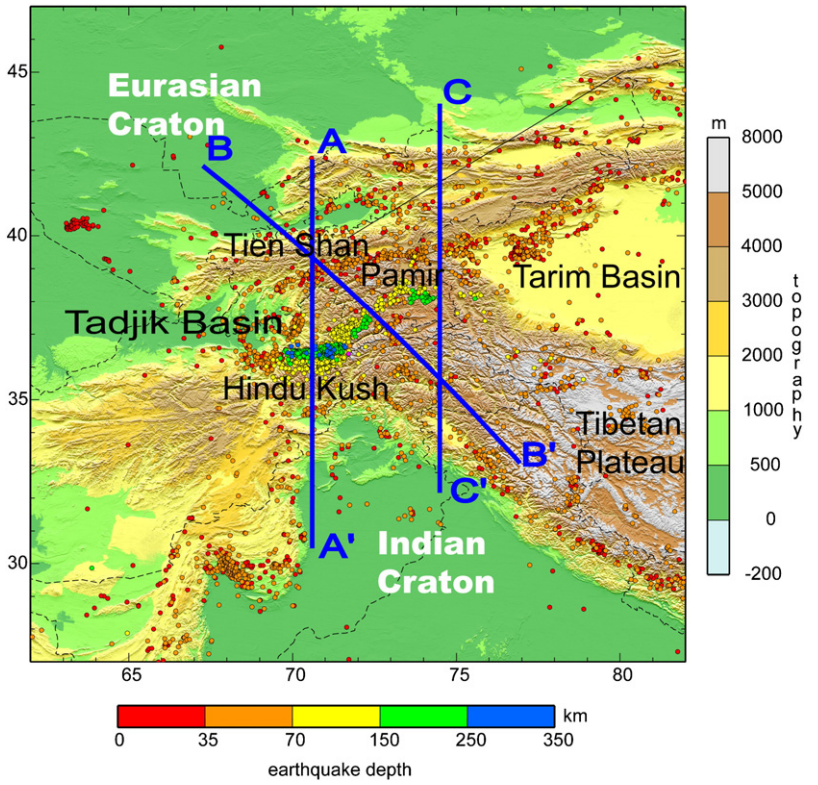

Fig. 1. Location map showing earthquakes occurred in the time period 1964–2002 that are listed in the bulletins of the International Seismological Centre (ISC) and have been relocated using the EHB methodology (Engdahl et al., 1998). Only earthquakes with formal uncertainties in epicenter smaller than 15 km are shown.

caused by a single, highly contorted slab (Billington et al., 1977; Vinnik et al., 1977). Pegler and Das (1998) relocated about 6000 shallow and intermediate-depth earthquakes in this area during the period 1964–1992 and provided a more detailed knowledge of the geometry of the seismic zone. They confirmed the earlier picture of a 700-km-long S-shaped seismic zone, and obtained that its width is generally less than 30 km. Despite this precise relocation study, the controversy about whether there is a single or two converging subduction zones could not be resolved using earthquake data alone. The tectonic context of the collision between India moving northwards and Asia suggests the presence of two converging subduction zones, with steep northward subduction of Indian lithosphere beneath the Hindu Kush, and southward subduction of Asian lithosphere under the Pamir (Chatelain et al., 1980; Burtman and Molnar, 1993; Fan et al., 1994). Both slabs meet at the easternmost limit of the Hindu Kush, giving the appearance of a laterally continuous subduction zone.

The nature – oceanic or continental – of the subducted lithosphere has also been a matter of debate when only earthquake data have been considered. The reduced width of the zone of intermediate-depth seismicity has been interpreted as an indication for the subduction of a trapped oceanic basin (Chatelain et al., 1980; Pavlis and Das, 2000). However, subduction of continental lithosphere in the upper part of the Hindu Kush was proposed by Roecker (Roecker, 1982) based on the low seismic velocities near the seismic zone. Furthermore a number of geological studies show that there has not been oceanic crust in the entire area of the western syntaxis since the Late Cretaceous (e.g. Burtman and Molnar, 1993; Hildebrand et al., 2001; Guillot et al., 2003). Also for the Pamir region, several studies provide geological and geophysical evidence for subduction of Eurasian continental lithosphere beneath the Pamir (Burtman and Molnar, 1993; Fan et al., 1994).

In this study we use tomographic images and seismicity distribution to infer the geometry of subduction beneath the Hindu Kush and Pamir regions. Then, based on tectonic reconstructions, we constrain the timing and rate of the subduction processes. This combination of tomography, seismicity and geologic reconstructions provides the input data required for 2D

thermal and rheological modeling of subduction carried out in this study.

2. Mantle structure in the Pamir–Hindu Kush region

We analyze three vertical cross-sections of the P-wave global tomographic model of Villaseñor et al. (Villaseñor et al., 2003) (Fig. 2) that run perpendicular to the strike of intermediate depth seismicity in the Pamir and Hindu Kush seismic regions (see Fig. 1 for location). The tomographic model has been obtained using the same method described in Bijwaard et al. (Bijwaard et al., 1998), but using a much larger dataset of arrival times of earthquakes listed in the bulletins of the International Seismological Centre (ISC) reprocessed using the EHB methodology (Engdahl et al., 1998).

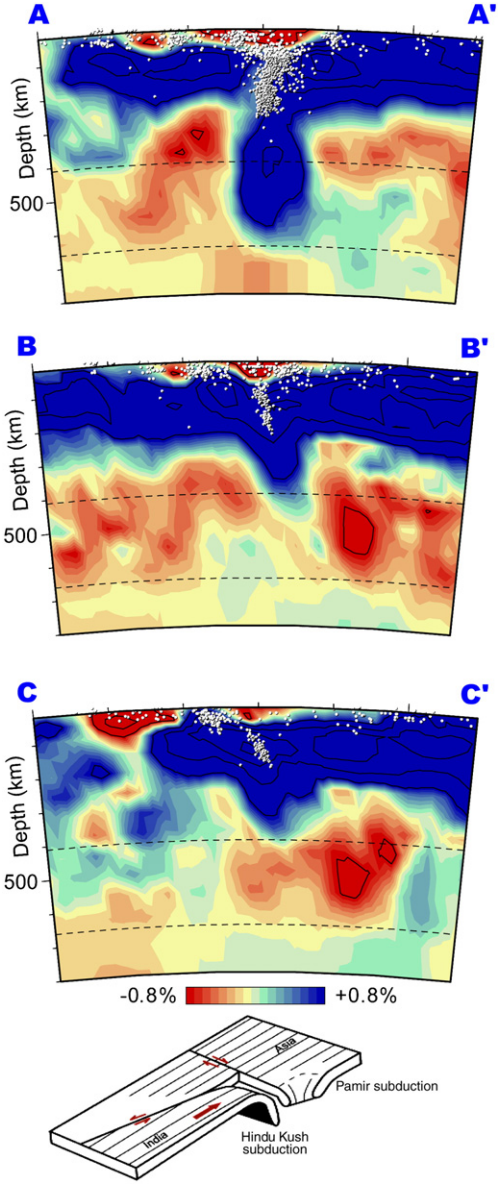

Fig. 2. Vertical cross-sections of the global P-wave tomographic model of Villaseñor et al. (2003) through the Hindu Kush and Pamir regions. See Fig. 1 for location. The contour interval is 1%. The inset at the bottom illustrates the multi-subduction 3-D geometry in the region (modified from Mattauer Mattauer, 1986).

Resolution of global travel-time tomography models with a large number of models parameters like the one presented here cannot be estimated quantitatively using the resolution matrix because the inversion is carried out using iterative methods (e.g. LSQR). Therefore we use the so-called "checkerboard tests" (reconstruction of synthetic models) to obtain a qualitative estimate of the resolution. The results of these tests are directly related to the amount of rays that crisscross in different azimuths each cell of the model. Because the study region exhibits a high level of seismicity, we expect good resolution. The tests results are good at all depths, and the quality of the reconstruction at 440 and 710 km is similar, indicating that there is not a significant deterioration of the resolution from the upper mantle to the transition zone.

Vertical cross-section AA′ shows that under the Hindu Kush region, the northwards subducting Indian plate is imaged throughout the upper mantle and transition zone, in agreement with other tomographic studies (Van der Voo et al., 1999; Koulakov and Sobolev, 2006). This vertical section indicates a thinning of the high velocity anomaly at depths of about 250 km, which has been interpreted as a progressive developing slab break-off (Koulakov and Sobolev, 2006). As mentioned before, there is no significant deterioration of spatial resolution in the upper mantle in the tomographic images. Therefore, the observed thinning of the high-velocity anomaly near 250 km depth is not related to a possible apparent broadening of the anomaly below this depth due to deteriorating resolution. Further to the NE, as entering the Pamir (section BB′), the slab imaged by high P-wave velocity anomaly dips to the SW and reaches shallower depths than the Hindu Kush slab. Across the eastern-most part of the Pamir region (vertical section CC′) the slab plunges southwards, with a shallower dip of both the seismic zone and of the high P-wave velocity anomaly. In order to better illustrate the multi-subduction 3D geometry of the area we show in Fig. 2 (inset at the bottom) a simplified sketch. The three tomographic vertical cross-sections show that the seismically active portion of the slabs is shallower than the extent of the

imaged slabs, in agreement with previous tomographic images of this region (Van der Voo et al., 1999; Koulakov and Sobolev, 2006).

Van der Voo et al. (Van der Voo et al., 1999), based on a N–S tomographic vertical cross-section across the Pamir at a longitude of about 73°E, proposed that the Indian slab presents a roll-over structure with the deeper portion overturned and dipping southward. Given that the cross-section shown by Van der Voo et al. (1999) is oriented somewhat obliquely to the strike of both intermediate seismicity and high-velocity anomalies in the mantle, it could be affected by three-dimensional geometric effects and could be possibly mapping the Asian slab above the transition zone and the Indian slab at deeper depths.

3. Constraints on subduction processes in the Hindu Kush and Pamir regions

Tomographic vertical cross-sections AA′ and CC′ are assumed to be representative of the geometry of the Indian slab under the Hindu Kush, and of the Asian slab under the Pamir, respectively. In this section, we combine the present-day geometry of the Hindu Kush slab with tectonic reconstructions, to infer additional constraints on the subduction process, in particular concerning the timing of initiation of subduction. In contrast, our inferences for the timing of initiation of subduction under the Pamir, are based on previous geological studies. These constraints will be useful to deduce the input parameters for the thermo-kinematic and rheological modeling described in Section 4.

3.1. Indian subduction beneath the Hindu Kush

Along the tomographic cross-section AA′, the Indian slab can be represented in the upper mantle by a simple geometry: to the south a horizontal segment starting at the frontal thrust position, to the north a vertical one, and a quarter of a circumference for the curved portion connecting both segments (Fig. 3). Then, we can unbend the slab to the horizontal position (blue box in Fig. 3), to obtain the length of the Indian continental lithosphere before subduction along this cross-section. We interpret this length as ‘a posteriori’ constraint of the size of India in the western part of the collision zone after the slab break-off process that most likely occurred at the early stage of the collision (e.g., Guillot et al., 2003; Chemenda et al., 2000; Kohn and Parkinson, 2002). This break-off had already been proposed in different seismic tomography studies (Van der Voo et al., 1999; Kárason, 2002) based on the lack of vertical continuity of high wave speed anomalies between the lower and upper mantle. Replumaz et al. (2004) interpret the long

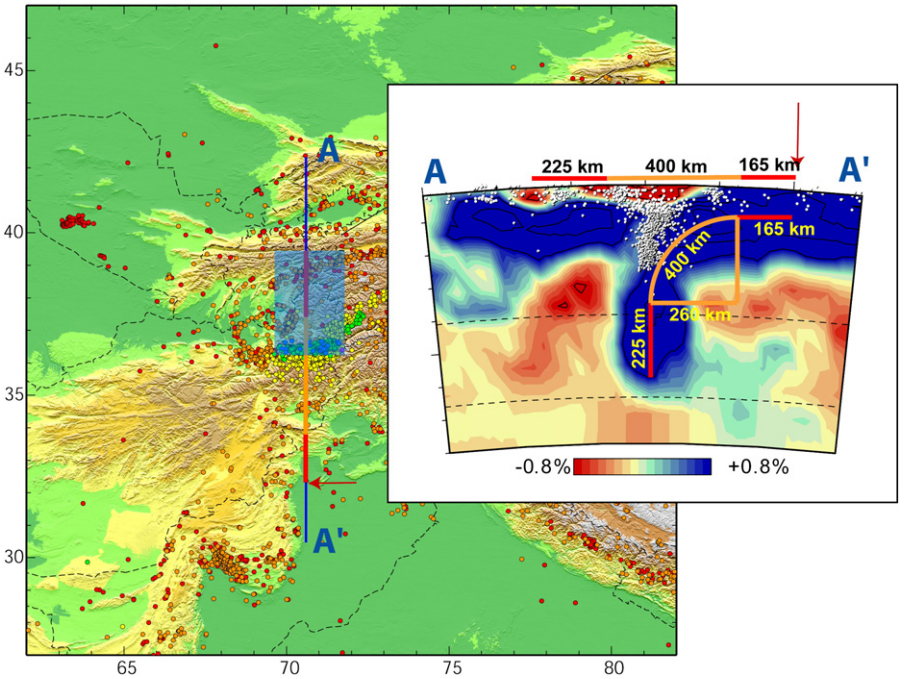

Fig. 3. Measurement of the length of the Indian slab under the Hindu Kush. The slab is then rolled up to horizontal (blue box in the map) to constrain the size of India in this area. The contour interval is 1%.

continuous NW–SE trending high wave speed anomaly at a depth of 1100 km, which remains nearly constant down to 1500 km, as marking the location of late Mesozoic oceanic subduction. West of 95°E this slab anomaly attenuates and vanishes between 1100 km and 800 km depth (Van der Voo et al., 1999; Kárason, 2002), thus indicating the geometry and the lateral extent of the slab break-off (Replumaz et al., 2004). It can therefore be inferred that the slab break-off occurred roughly at the same time all along the northern limit of continental India, and it represents the transition between the stable oceanic subduction, and a more contorted and laterally disrupted continental subduction. A larger tomographic vertical cross-section containing section AA′ is shown in Fig. 4 to illustrate both the interruption of the slab between 1100 km and 600 km depth, and the continuity of the Indian slab after the break-off.

Following Replumaz et al. (2004), we use a reference frame attached to present-day Siberia to interpret the mantle structures, based on the small motion of Asia with respect to the hotspot reference frame. The position of the slab at approximately 1100 km depth on tomographic images would correspond to the position of the subduction zone at the time of slab break-off. This slab anomaly location is successfully matched by the geologically reconstructed position of the Asian plate boundary at 40–50 Ma (Replumaz et al., 2004), thus providing a first order estimate of the age of slab break-off along the collision zone. We draw the corresponding northern limit of India north of the high wave speed anomaly, since the slab break-off most probably occurred while India began to override its own sinking slab, and thus the rupture zone is most probably located north of the anomaly (Fig. 5). The southern limit of India is given by the position deduced by Patriat and Achache (Patriat and Achache, 1984) using the oceanic magnetic anomalies in the central Indian Ocean (Fig. 5). We test several positions of India assuming different anomaly times: 18 (41.81 Ma), 20 (44.4 Ma) and 21 (47.69 Ma). The area between the northern and southern margins corresponds to the total extent of India, at the time of slab break-off, being the northern margin involved afterwards in the collision process (Fig. 5). The total extent of India deduced in this way must be compared with that deduced from the horizontal restoration of the slab imaged beneath the Hindu Kush (Fig. 3). To perform this comparison we rotate India on the sphere back to present about the Euler poles of India–Eurasia relative motion given by Patriat and Achache (Patriat and Achache, 1984). This comparison reveals that a good match of the tomographically inferred size of India (after slab break-off) in the

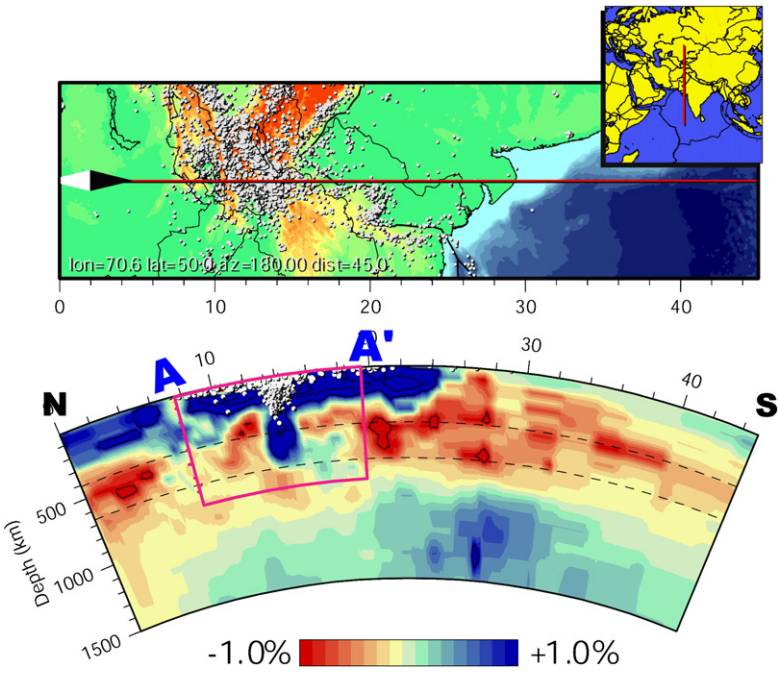

Fig. 4. Vertical tomographic cross-section that includes section AA′ (pink box), and shows the lack of vertical continuity of high velocity anomalies from the lower to the upper mantle, which is interpreted as an evidence of slab break-off. The contour interval is 1%.

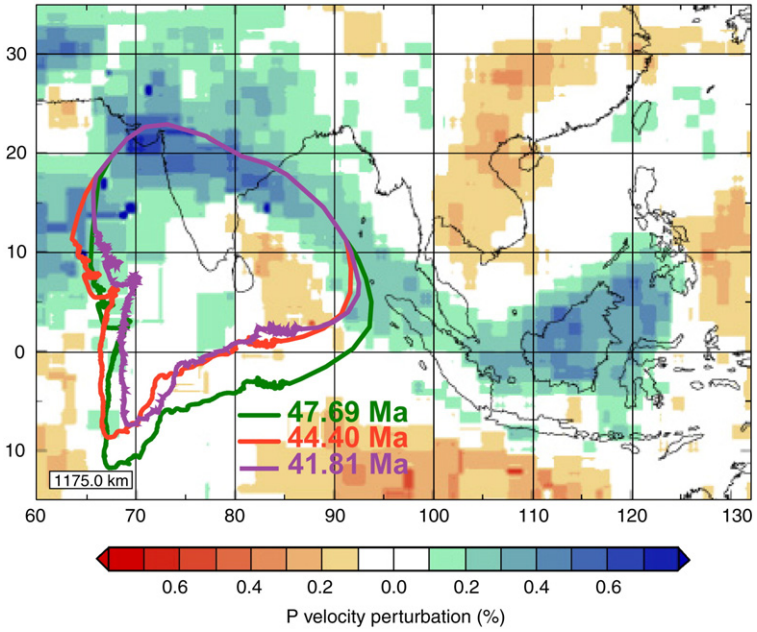

Fig. 5. Horizontal tomographic section at 1175 km depth. The long NW–SE trending high velocity anomaly is assumed to mark the position of the northern boundary of India at the time of slab break-off. For the southern limit we test different positions of India deduced by Patriat and Achache (Patriat and Achache, 1984) using the oceanic magnetic anomalies in the central Indian Ocean.

Hindu Kush zone is only obtained when considering the magnetic anomaly 20 (44.4 Ma) (Fig. 6). We have performed a test where, instead of considering the northern end of the high wave speed anomaly, we draw

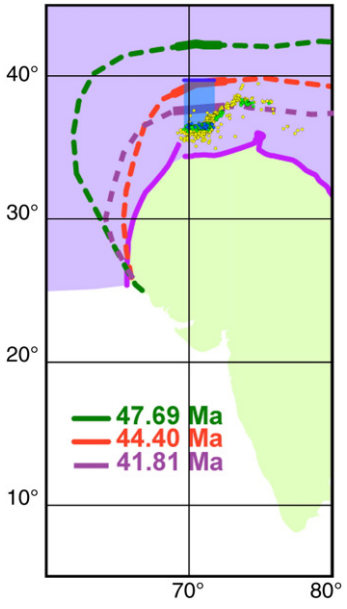

Fig. 6. Comparison between the horizontal projection of the Indian slab under the Hindu Kush and the positions of the inferred northern boundary of India after rotating it to present about Euler poles given by Patriat and Achache (Patriat and Achache, 1984).

the northern boundary of India along the southern end of the anomaly. A good match of the length of the slab is then obtained considering the anomaly 21 (47.69 Ma). Therefore, we estimate an age of slab break-off of about 44–48 Ma. This age is in good agreement with the age of late Eocene K-rich magmatism observed in south-eastern Tibet, which appears to be related to the Indian slab break-off (Kohn and Parkinson, 2002), and with the results of the thermomechanical laboratory modeling of continental subduction by Chemenda et al. (Chemenda et al., 2000). These authors suggest that a break-off of Indian lithosphere with attached previously subducted oceanic lithosphere occurred some 45 Ma ago. Actually, since the estimated age of the initial contact between the Indian and Asian continental margins ranges between 58 and 55 Ma depending on the type of data used (e.g. Guillot et al., 2003; Leech et al., 2005 and references therein), this break-off process most probably detached also a portion of continental lithosphere. It must be kept in mind the uncertainties regarding the lateral extent of this initial contact, specially considering the large number of proposals for the geometry of 'Greater India', that is, the Indian subcontinent plus a postulated northern extension (see Ali and Aitchison, 2005 for a compilation and revision of proposals). Therefore, in principle, one should accept the possibility that the Indian margin in the Hindu Kush was still oceanic and that the actual 'contact' was much later in the western

part of the collision zone. However, the main evidences in favor of an earlier continental contact come from a number of geological studies of the Pamir, Hindu Kush, and Tadjik Basin that demonstrate that there has been no oceanic crust in the region since at least the Late Cretaceous (e.g. Burtman and Molnar, 1993; Hildebrand et al., 2001; Guillot et al., 2003).

Concerning the location and timing of initiation of present-day Indian continental subduction beneath the Hindu Kush, a first scenario consists of assuming that subduction began immediately after slab break-off and progressively migrated towards the north, reaching its present-day location. However, such evolution would probably result in a slab overturned beneath India. Furthermore, the steepness of the slab beneath the Hindu Kush suggests that the location of this continental subduction is stable through time. This is observed for the subduction zone surrounding Southeast Asia, which appears stationary at the surface since 15 Ma (Replumaz and Tapponnier, 2003), and is also characterized by a steep slab. This correspondence between the stationary position of the convergent margin and the vertical slab led Replumaz et al. (Replumaz et al., 2004) to deduce that sinking of cold material occurred with little lateral advection in a mantle reference frame. We therefore infer that subduction initiated roughly at the same position as it is presently observed. As the present-day location of the Indian slab is at ~36°N (Fig. 1), this implies that after slab break-off that occurred at ~23°N (Fig. 5), western India continued its northward drift, pushing the Asian lithosphere to the north, until a segment of the northern boundary of India reached the present Hindu Kush seismic zone, where it began to subduct. Therefore, paleomagnetic reconstructions are needed again to constrain the timing of this second subduction process. We use the results of Patriat and Achache (Patriat and Achache, 1984) to obtain the amount of northward drift of the inferred northern boundary of India plate after slab break-off. Fig. 7 illustrates that this boundary reached the zone of present-day intermediate seismicity between 10 and 5 Ma. We conclude that the near vertical subduction presently observed in the Hindu Kush region began at around 8 Ma. Therefore a subduction velocity of about 5 cm yr^{-1} is required to reproduce the present-day length of the Indian slab. This means that, given a convergence rate between Eurasia and India of 5.0± 0.5 cm yr^{-1} during the last 20 Ma (DeMets et al., 1990; Bilham et al., 1997), all the recent convergence in the Hindu Kush region would be accommodated by subduction of the Indian lower crust and lithospheric mantle.

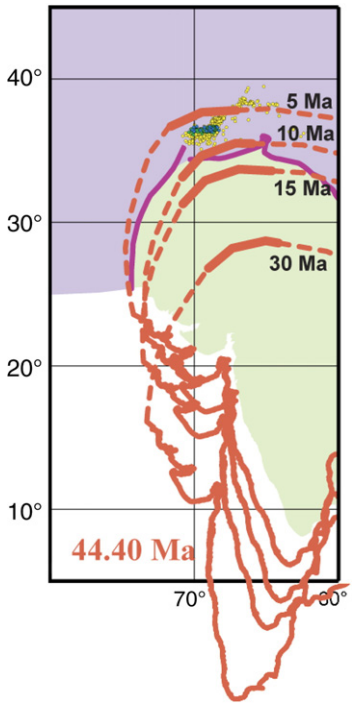

Fig. 7. Positions of India at different times, using the Euler poles by Patriat and Achache (Patriat and Achache, 1984) and considering that slab break-off occurred at about 44.4 Ma. The inferred northern boundary of India at the time of break-off is shown to reach the zone of present-day intermediate seismicity between 10 and 5 Ma.

3.2. Asian subduction beneath the Pamir

Further to the northeast, as entering the Pamir region, the high wave speed anomalies in the upper mantle are shallower and the dip of seismic zone gradually decreases from about 80° southeastward to about 45° southward (Fig. 2, cross-sections BB′ and CC′). Concerning the timing and amount of subduction in the Pamir region, the study by Burtman and Molnar (Burtman and Molnar, 1993) provides compelling geological and geophysical evidence for late Cenozoic subduction of a minimum of 300 km of Eurasian continental lithosphere beneath the Pamir. These authors show that the northern margin of the Pamir has been thrusted at least 300 km over southern Eurasia. This amount, together with a minimum of 300 km of Cenozoic crustal shortening within the Pamir (leading to a present crustal thickness of about 70 km), implies that the southern edge of the Pamir has moved northward at least 600 km with respect to the area further north. This amount of convergence is compatible with the image of the Asian slab in the cross-section CC′ reaching a depth of about 300–350 km along a 45° dipping plane. Concerning the nature and thickness of

the subducted crust, Burtman and Molnar (Burtman and Molnar, 1993) state that intermediate-depth earthquakes occur in a lithosphere that once underlaid the sediments now folded in the Pamir–Altai zone. Since these sediments were scraped off the crust that once laid east of the Tadjik basin, by analogy with the crust beneath this basin, Burtman and Molnar (Burtman and Molnar, 1993) infer a crustal thickness of 20–25 km.

4. Thermo-kinematic and rheological modeling

4.1. Thermal modeling

The temperature distribution within the slab and surrounding mantle is calculated using the TEMSPOL code (Negredo et al., 2004). This code allows the calculation of temperature and density anomaly distributions in deep subduction zones, taking into account self-consistently the olivine to spinel phase transformation. The code adopts a finite difference scheme to solve the heat transfer equation

$$\left(1+\frac{L_T}{c_p}\frac{\partial\beta}{\partial T}\right)\left(\frac{\partial T}{\partial t}+v_x\frac{\partial T}{\partial x}+v_z\frac{\partial T}{\partial z}\right) = \frac{K}{\rho c_p}\left(\frac{\partial^2 T}{\partial x^2}+\frac{\partial^2 T}{\partial z^2}\right)-v_z\left(\frac{\alpha g}{c_p}T_{abs}+\frac{L_T}{c_p}\frac{\partial\beta}{\partial z}\right)+\frac{H+A_{sh}}{\rho c_p} \quad (1)$$

where L_T is the latent heat due to the olivine–spinel transformation, c_p is the heat capacity, β is the fraction of spinel, T is the temperature, t is time, x and z are the coordinates, v_x and v_z are the horizontal and vertical components of the velocity, K is the thermal conductivity, ρ is the density, α is the coefficient of thermal expansion, g is the acceleration of gravity, T_{abs} is the absolute temperature, H is the radiogenic heat production rate, and A_{sh} is the shear heating rate. The values of the parameters common to all calculations are listed in Table 1. Neither shear heating nor radiogenic production are considered in the calculations.

Table 1
Common parameters used in calculations

Symbol	Meaning	Value
K	Thermal conductivity	3.2 W m^{-1} K^{-1}
c_p	Specific heat	1.3×10^3 J K^{-1} kg^{-1}
α	Thermal expansion coefficient	3.1×10^{-5} K^{-1}
ρ_0	Reference density of the mantle	3400 kg m^{-3}
g	Gravitational acceleration	9.8 m s^{-2}
L_T	Latent heat of olivine–spinel transformation	90 kJ kg^{-1}

The terms on the left side of Eq. (1) represent the rate of heat change due to the temperature change at a fixed point and advection. The first term on the right side represents heat conduction, the term containing T_{abs} describes the adiabatic heating, the term containing L_T represents the latent heat of the olivine to spinel transformation, and the last term accounts for radiogenic and dissipative heating. The initial thermal distribution of the oceanic lithosphere is calculated with the thermal plate model GDHI of Stein and Stein (Stein and Stein, 1992). The code also includes the possibility of simulating continental subduction, with an initial geotherm for the crust and lithospheric mantle given by the steady-state solution of the heat conduction equation. We assume an adiabatic initial temperature profile for the asthenosphere. We also include a total temperature increase $\Delta T=L_T/c_p$, caused by the latent heat released during the olivine to spinel phase change (Turcotte and Schubert, 2002).

To compute the fraction of 'spinel' – representing both wadsleyite (β) and ringwoodite (γ) – and its derivatives at any temperature and depth, we follow the approach described by Schmeling et al. (1999) of adopting a simplified phase diagram, from original data by Akaogi et al. (1989) and Rubie and Ross (1994). The effects of potential olivine metastability at temperatures below 600 °C are included in the phase diagram used.

In our thermo-kinematic approach the velocity field is imposed and defined by the subduction velocity and the slab dip. This modeling procedure shares many characteristics with the thermal model by Minear and Toksöz (1970). The velocity field is updated as the slab penetrates into a static mantle. We apply the Alternating Direction Implicit (ADI) method for the finite difference formulation of the energy equation (Eq. (1)). The reader is referred to Negredo et al. (2004) for further details about modeling procedure, numerical method and TEMSPOL code availability.

For the sake of simplicity, we have followed the classical approach of assuming a plate-like behaviour for downwelling slab. This approach is commonly used in the literature to model subduction processes in specific areas (e.g. Hafkenscheid et al., 2001). An alternative type of model to study downwelling of mantle material in convergent continental settings is based on the idea of continuum viscous flow of an unstable mantle layer. Billen and Houseman (2004) apply this kind of dynamic approach to the San Gabriel mountains in Southern California. Provided that the main characteristics of our study area (deep high wave speed anomaly and intermediate-depth seismicity describing a relatively well defined Wadatti–Benioff

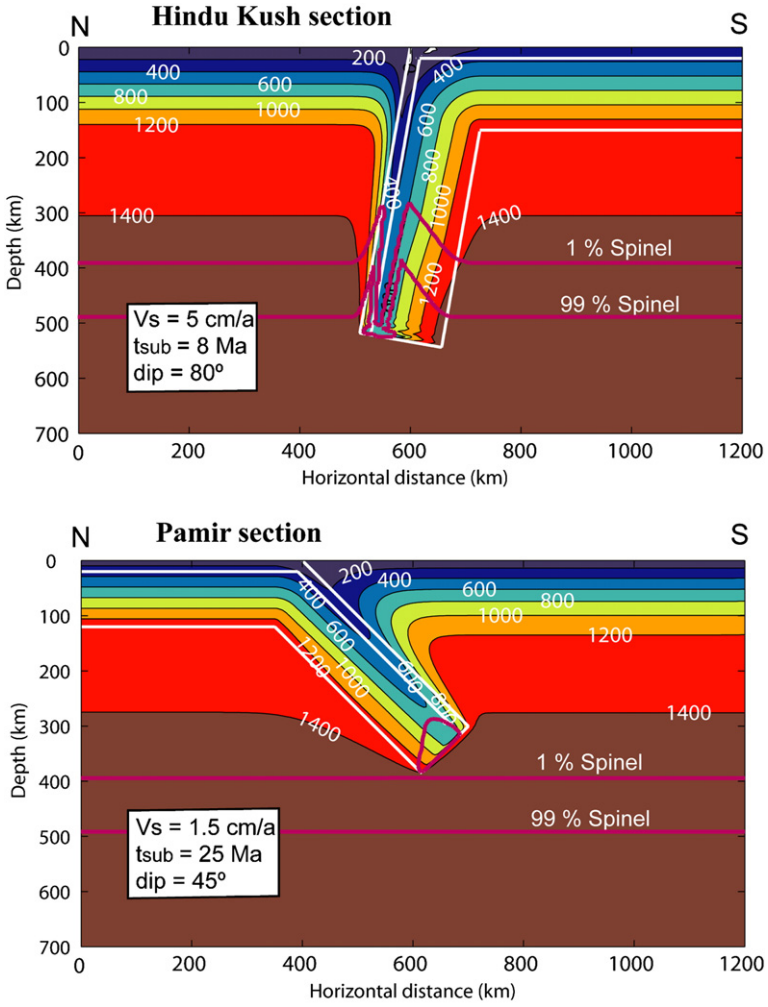

Fig. 8. Temperature (°C) distributions predicted in both modeled sections. Higher imposed velocity of subduction under the Hindu Kush leads to lower slab temperatures than under the Pamir.

zone) are typical of a subduction process, we have preferred to adopt a thermo-kinematic approach adequate to model continental and oceanic subduction processes.

The geometric and kinematic parameters adopted in the modeling are consistent with the observations described in the previous sections. Vertical tomographic cross-sections (Fig. 2) are used to constrain the slab depth, thickness and dip. The thermal modeling of the subduction zone beneath the Hindu Kush assumes a 150-km-thick Indian continental slab dipping 80°. We also assume that the slab contains a 20-km-thick crustal layer representing the lower crust, whereas the more buoyant upper crust has been accreted to the Hindu Kush belt. This subducting lower crust is assumed to be converted to eclogite, so that its density is increased and becomes less buoyant. As previously discussed, we consider a subduction velocity of about 5 cm yr^{-1}. Temperatures of 200 °C and 1350 °C are imposed at the top and base of the subducting plate, respectively. The first value is assumed to be representative of the temperature at the limit between upper and lower crust, given the thickness and basal temperature considered for the subducting plate.

The tomographically inferred length of the Asian slab under Pamir is of about 400 km (measured from the outer Pamir arc; cross-section CC′ in Fig. 2). The paleomagnetic reconstructions of the position of the outer Pamir arc at the beginning of Neogene time produced a location of at least 300 km south of its present location (Burtman and Molnar, 1993). This distance of 300 km roughly corresponds to the horizontal projection of the Asian slab under Pamir, considering a subduction dip of 45°. Therefore, we

assume that subduction began at about 25 Ma, and the velocity of subduction required to produce a 400-km-long slab is then calculated to be of a minimum of 1.5 cm yr^{-1}. The assumed plate thickness is 120 km, comprising a 20-km-thick crust (Burtman and Molnar, 1993), with top and bottom temperatures of 0 °C and 1350 °C, respectively.

The temperature distributions obtained for both subduction zones are shown in Fig. 8. Isotherms are more depressed within the slab under the Hindu Kush than under the Pamir, due to the higher subduction rate in the former region (5 cm yr^{-1} vs. 1.5 cm yr^{-1}). A limitation of this modeling approach is that the slab is assumed to penetrate into a static mantle; therefore we disregard possible effects of flow induced in the mantle wedge between the top of the slab and the overriding plate. As a consequence, the temperatures predicted near the slab–wedge interface can be significantly underestimated (e.g. Van Keken et al., 2002).

Some authors convert the temperature distribution predicted with similar models into seismic velocity anomalies (e.g. Hafkenscheid et al., 2001). However, it is well known that travel time tomography (seismic tomography using arrival times of body waves) underestimates the values of the seismic anomalies. Therefore, in this study we only make use of the geometry of the high-velocity seismic anomalies associated with subducting slabs, and not of the values of the anomalies. For this purpose we should use other types of tomographic models, such as those obtained from long period body and surface waves and normal modes.

Fig. 8 also shows the location of the olivine–spinel (1% and 99% spinel curves) transformation. In the case of the model simulating subduction under the Hindu Kush, the 600 °C isotherm, which controls the initiation of metastable olivine to spinel transformation, reaches maximum depths of about 500 km, so the conditions for the formation of a small wedge of mestastable olivine in the transition zone are attained. Taking into account a number of studies suggesting that deep focus earthquakes are caused by shear instabilities associated with olivine to spinel transformation in metastable olivine wedges (Green et al., 1990; Kirby et al., 1991; Kirby et al., 1996), we deduce from our results that earthquakes at depths greater than 300 km in the Hindu Kush region could be associated with the presence of metastable olivine at these depths. In contrast, the warmer slab under the Pamir does not reach the conditions for metastability, and a shallowing of the curve representing the initiation of olivine to spinel transformation in the slab is predicted.

4.2. Rheological modeling

Once the temperature distribution is obtained, we use the rheological modeling procedure applied by Carminati et al. (2005) to evaluate the extent of brittle regions in subduction zones. We calculate at each grid node the brittle and ductile yield stress imposing a posteriori the rheological laws. The brittle yield stress is obtained by applying the Sibson's law (Sibson, 1981), which is based on the Coulomb–Navier frictional criterion and predicts a linear increase with depth of yield stress:

$$\sigma_1 - \sigma_3 = \beta \rho g z (1 - \lambda) \tag{2}$$

where β is a parameter depending on the fault type, ρ is the density, g is the gravity acceleration, z is the depth and λ is the pore fluid pressure ratio (i.e., the ratio between fluid pressure and lithostatic load). We use here the same choice of parameters as Carminati et al. (2005): β parameter is assumed as 3 and the average density $\rho = 3200$ kg m^{-3}. The fluid pressure is assumed to be hydrostatic ($\lambda = 0.4$).

For the ductile behavior we adopt the following power law creep relation,

$$\sigma_1 - \sigma_3 = \left(\frac{\dot{\varepsilon}}{A}\right)^{1/n} \exp\left(\frac{Q}{nRT}\right) \tag{3}$$

where $\dot{\varepsilon}$ is the effective strain rate, A is the generalized viscosity coefficient, n is the stress power law exponent, Q is the activation energy, R is the gas constant and T is the absolute temperature. Due to the simple kinematic approach adopted in this modeling, where the velocity field is imposed, the distribution of strain rate is not computed. Therefore, we assume a strain rate value constant throughout the model domain, and we compute resistance opposed to deformation with that given strain rate. We perform sensitivity tests varying the imposed strain rate between 10^{-15} and 10^{-13} s^{-1}.

The ductile strength of the continental crust is calculated assuming quartzdiorite rheological parameters down to depths of 40 km: $A = 0.0013$ MPa^{-n} s^{-1}, $n = 2.4$, $Q = 219$ kJ mol^{-1} (Ranalli, 1997). At greater depths, we adopt the values $A = 0.00017$ MPa^{-n} s^{-1}, $n = 3.25$, $Q = 248$ kJ mol^{-1} calculated by Carminati et al. (2002) for high pressure–low temperature metamorphosed crustal rocks. We assume a dunitic continental lithospheric mantle with the following rheological parameters: $A = 2000$ MPa^{-n} s^{-1}, $n = 4$, $Q = 471$ kJ mol^{-1} (Ranalli, 1997).

After computing at each grid node the brittle and ductile yield stresses, the lesser of both is considered to be the differential yield stress required to produce failure

at that point (Goetze and Evans, 1979). Therefore, the brittle field is defined by nodes with brittle strength lower than ductile strength, and the opposite stands for the ductile domain. Provided that seismicity down to depths of about 300 km is likely produced by rupture within the brittle field, we will analyze whether earthquake distribution both in the Pamir and Hindu Kush slabs correlates well with the calculated brittle field.

Fig. 9 shows the influence of strain rate on the brittle–ductile transition depth. Deeper transition depths are predicted for increasing strain rates because of the increase of ductile yield stress (Eq. (3)). A brittle behavior is predicted down to depths of about 380 km in the mantle portion of the slab and down to 200 km in the crustal portion. Carminati et al. (2005) investigated the influence of the assumed brittle strength distribution. In addition to the Sibson law with $\lambda=0.4$ used in the present study, these authors also considered the effects of fluid overpressures caused by dehydration processes (i.e. Sibson law with $\lambda>0.4$), and of constant brittle strength at high pressures (Shimada, 1993). They obtained the shallowest brittle–ductile transition with the Sibson law for $\lambda=0.4$. This means that the high maximum depth for brittle behavior predicted for the Hindu Kush zone would be even higher with other brittle strength distributions. We can therefore infer that the observed distribution of intermediate seismicity within the Hindu Kush slab is consistent with the down-dip extent of the brittle portion of the slab predicted for high subduction rates. In particular, the relatively large depth and narrowness of the Hindu Kush seismic zone

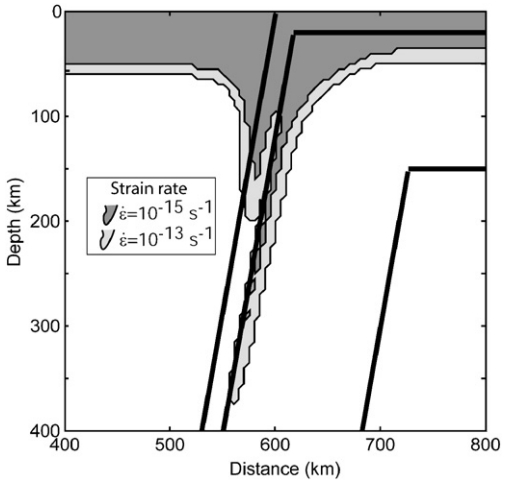

Fig. 9. Influence of the strain rate on the brittle–ductile transition depth predicted for the Indian slab under the Hindu Kush. A brittle behavior is predicted down to depths of about 320 km.

are two prominent characteristics reproduced by our modeling.

Some areas of predicted brittle behavior would require unrealistic high differential stresses to produce faulting. These stresses would be significantly reduced in case of dehydration ($\lambda>0.4$ in the Sibson law), thus promoting brittle failure and earthquakes (see discussion in Carminati et al., 2005, and references therein).

In order to evaluate the sensitivity of our results to kinematic parameters, we tested some models with a subduction velocity as low as 1.5 cm yr^{-1}, the value assumed for subduction under the Pamir, and obtained a decrease of maximum brittle–ductile transition depth to 240 km (with exactly the same final configuration, rheological parameters and strain rate of 10^{-15} s^{-1}). In addition, taking into account the large uncertainties regarding the choice of rheological parameters for creep, we performed a comparison between the results shown so far with parameters representative for a continental slab, and the results obtained with the following parameters adequate for a typical oceanic slab. The crust is assumed to be composed of diabase down to 40 km, with parameters: $A=2\times10^{-4}$ MPa^{-n} s^{-1}, $n=3.4$, $Q=260$ kJ mol^{-1} (Liu and Furlong, 1993). At depths greater than 40 km, the crust is assumed to be eclogitized, due to high pressure–low temperature metamorphism. We assume a mineral composition of eclogite consisting of 60% clinopyroxene and 40% garnet, and corresponding parameters: $A=2430$ MPa^{-n} s^{-1}, $n=2.6$ and $Q=449$ kJ mol^{-1} (Ji and Zhao, 1994). We assume a harzburgitic composition for oceanic lithosperic mantle, and adopt the following parameters: $A=1010$ MPa^{-n} s^{-1}, $n=2.4$, $Q=367$ kJ mol^{-1} (Ji and Zhao, 1994). In the case of modeled oceanic slab, the crustal thickness was assumed to be 10 km, instead of the 20 km assumed for the continental slab. The rest of parameters are exactly the same as in Fig. 9 with a strain rate of 10^{-15} s^{-1}. Fig. 10 shows the results of this comparison, that reveals that the maximum brittle–ductile transition depth does not increase significantly, but the brittle portion of the slab becomes wider. The main difference is that the brittle region of the crust in the slab is deeper for an eclogitic composition since ductile strength is increased. Therefore, if we considered a continental slab containing eclogitized lower crust, as proposed in this region by Searle et al. (2001), most of intermediate depth earthquakes would probably occur within the crust, instead of in the lithospheric mantle.

The same comparison between assumed continental and oceanic compositions is performed for the slab under the Pamir (Fig. 10). A constant strain rate of 10^{-15} s^{-1} is assumed. Expectedly, the predicted brittle–

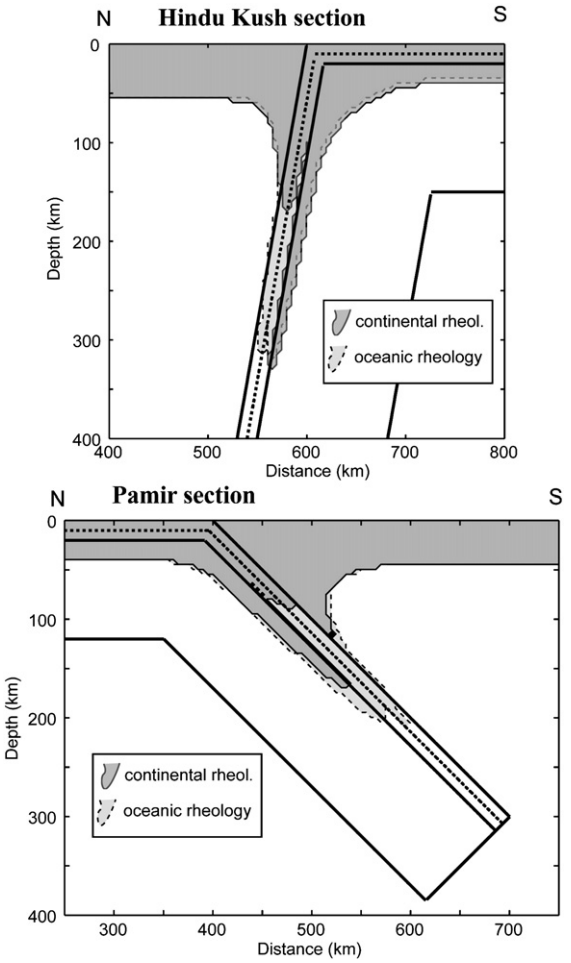

Fig. 10. Predicted brittle fields considering typical parameters for continental and oceanic rheology. Lower temperatures under the Hindu Kush lead to a deeper brittle region than under the Pamir.

ductile transition depths are much shallower than those predicted for the faster (therefore colder) slab under the Hindu Kush, in good agreement with the much shallower intermediate-depth seismicity in the Pamir. Again, the uncertainties concerning the composition and adequate rheological parameters for the subducted crust precludes to infer whether intermediate depth earthquakes occur mostly in the crust or in the lithospheric mantle. These results illustrate that, independently from the assumed composition, the differences in depth reached by intermediate-depth seismicity are largely related to the different thermal distributions within both slabs, which are mainly controlled by the different subduction rates, whereas the assumed compositions play a secondary role.

This thermo-rheological modeling shows that faster subduction under the Hindu Kush than under the Pamir is required to explain the greater depth of intermediate-depth seismicity beneath the first region. Therefore, this modeling gives further support to the idea of the presence of two converging subduction zones, instead of a single contorted one. It is worth noting that, keeping in mind the large uncertainties regarding the choice of the specific law assumed for brittle strength and of rheological parameters for creep, the predicted brittle–ductile transition depths should not be read literally (see Carminati et al., 2005 for detailed discussion). The purpose of these calculations is to illustrate that different subduction rates between the Pamir and Hindu Kush lead to different depths of the brittle region for both areas, rather than predicting accurate brittle–ductile transition depths.

This thermo-rheological modeling is consistent with our inferences form reconstructions discussed in the previous section, and with geologic studies (e. g. Searle et al., 2001) that propose similar ages for the initiation of continental subduction processes under the Hindu Kush.

5. Conclusions

In this study we have used tomographic images to constrain the geometry of slabs under the Hindu Kush and Pamir regions. The change of depth and dip of the slabs shows the same trend as seismicity: from steep northward dipping of the Indian slab under the Hindu Kush to southward dipping of a shallower Asian slab under the Pamir.

Provided that the lack of vertical continuity of high wave speed anomalies from the lower to the upper mantle is a clear evidence of slab break-off, the length of the Indian slab above the discontinuity is measured to give a constraint of the size of India after slab break-off. We consider different positions of India, at the time of break-off, given by different oceanic magnetic anomalies, and we obtain a good match of the inferred length of the Indian slab when considering the anomalies at 44.4 Ma and 47.69 Ma. In this way we deduce an age of slab break-off of about 44–48 Ma, in good agreement with previous studies.

We deduce that after slab break-off India followed its northward motion horizontally, until the northern boundary of India reached the present-day Hindu Kush region, where it began to subduct vertically some 8 Ma ago. A velocity of subduction under Hindu Kush as high as 5 cm yr^{-1} during the last 8 Ma is then required to reproduce the observed length of the Indian slab. This high velocity implies that all the recent convergence between India and Eurasia in the Hindu

Kush region would be accommodated by subduction of the Indian lower crust and lithospheric mantle.

Thermo-kinematic and rheological modeling indicates that the slower subduction rate under Pamir, deduced from previous geological studies (1.5 cm yr^{-1} under the Pamir vs. 5 cm yr^{-1} under the Hindu Kush), is responsible for the higher slab temperatures. This results in a shallower brittle region, which is consistent with shallower intermediate-depth seismicity than in the Hindu Kush region.

The large differences in the deduced velocities of subduction and ages of initiation of subduction in both regions provide further support to the presence of two converging subduction zones, instead of a single contorted one.

Acknowledgements

The authors are very grateful to three anonymous reviewers for their constructive revision of the manuscript. This study has been supported by projects CTM2006-13666-C02-02/MAR, CTM2005-08071-C03-03/MAR, and by the Consolider-Ingenio 2010 Programme (under project CSD2006-00041, "Topo-Iberia"). A.M.N acknowledges support from a Flores Valles-UCM grant for a six-month stay in the Université Lyon 1. A.V. has also been partially supported by ISES (Netherlands Research Center for Integrated Solid Earth Science).

References

Akaogi, M., Ito, E., Navrotsky, L., 1989. Olivine-modified spinel–spinel transitions in the system Mg_2SiO_4–Fe_2SiO_4: calorimetric measurements, thermochemical calculation and geophysical application. J. Geophys. Res. 94, 15671–15685.

Ali, J.R., Aitchison, J.C., 2005. Greater India. Earth-Sci. Rev. 72, 169–188.

Bijwaard, H., Spakman, W., Engdahl, E.R., 1998. Closing the gap between regional and global travel time tomography. J. Geophys. Res. 103, 30055–30078.

Bilham, R., Larson, K., Freymueller, J., 1997. GPS measurements of present-day convergence across the Nepal Himalaya. Nature 386, 61–64.

Billen, M.I., Houseman, G.A., 2004. Lithospheric instability in obliquely convergent margins: San Gabriel Mountains, southern California. J. Geophys. Res. 109, B01404. doi:10.1029/2003JB002605.

Burtman, V.S., Molnar, P., 1993. Geological and geophysical evidence for deep subduction of continental crust beneath the Pamir. Spec. Pap.-Geol. Soc. Am. 281 (76 pp.).

Billington, S., Isacks, B.I., Barazangi, M., 1977. Spatial and focal mechanisms of mantle earthquakes in the Hindu Kush–Pamir region: a contorted Benioff zone. Geology 5, 699–704.

Carminati, E., Giardina, F., Doglioni, C., 2002. Rheological control on subcrustal seismicity in the Apennines subduction (Italy). Geophys. Res. Lett. 29, doi:10.1029/2001GL014084.

Carminati, E., Negredo, A.M., Valera, J.L., Doglioni, C., 2005. Subduction-related intermediate-depth and deep seismicity in Italy: insights from thermal and rheological modeling. Phys. Earth Planet. Inter. 149, 65–79.

Chatelain, J.L., Roecker, S.W., Hatzfeld, D., Molnar, P., 1980. Microearthquake seismicity and fault plane solutions in the HinduKush region and their tectonic implications. J. Geophys. Res. 85, 1365–1387.

Chemenda, A.I., Burg, J.P., Mattauer, M., 2000. Evolutionary model of the Himalaya–Tibet system: geopoem based on new modeling, geological and geophysical data. Earth Planet. Sci. Lett. 174, 397–409.

DeMets, C., Gordon, R.G., Argus, D.F., Stein, S., 1990. Current plate motions. Geophys. J. Int. 101, 425–478.

Engdahl, E.R., van der Hilst, R., Buland, R.P., 1998. Global teleseismic earthquake relocation with improved travel times and procedures for depth determination. Bull. Seismol. Soc. Am. 88, 3295–3314.

Fan, G., Ni, J.F., Wallace, T.C., 1994. Active tectonics of the Pamirs and Karakorum. J. Geophys. Res. 99, 7131–7160.

Goetze, C., Evans, B., 1979. Stress and temperature in the bending lithosphere as constrained by experimental rock mechanics. Geophys. J. R. Astron. Soc. 59, 463–478.

Guillot, S., Garzanti, E., Baratoux, D., Marquer, D., Mahéo, G., de Sigoyer, J., 2003. Reconstructing the total shortening history of the NW Himalaya. Geochem. Geophys. Geosyst. 4, 484–506.

Green, H.W., Young, T.E., Walker, D., Scholz, C.H., 1990. Anticrack-associated faulting at very high pressure in natural olivine. Nature 348, 720–722.

Hafkenscheid, E., Buiter, S.J.H., Wortel, M.J.R., Spakman, W., Bijwaard, H., 2001. Modelling the seismic velocity structure beneath Indonesia: a comparison with tomography. Tectonophysics 333, 35–46.

Hildebrand, P.R., Noble, S.R., Searle, M.P., Waters, D.J., Parrish, R.R., 2001. Old origin for an active mountain range: geology and geochronology of the eastern Hindu Kush, Pakistan. Geol. Soc. Am. Bull. 113, 625–639.

Ji, S., Zhao, P., 1994. Layered rheological structure of subducting oceanic lithosphere. Earth Planet. Sci. Lett. 124, 75–94.

Kárason, H., 2002. Thesis, Massachusetts Institute of Technology, Cambridge, MA.

Kirby, S.H., Durham, W.B., Stern, L.A., 1991. Mantle phase changes and deep–earthquake faulting in subducting lithosphere. Science 252, 216–225.

Kirby, S.H., Stein, S., Okal, E., Rubie, D.C., 1996. Metastable mantle phase transformations and deep earthquakes in subducting oceanic lithosphere. Rev. Geophys. 34, 261–306.

Kohn, M.J., Parkinson, C.D., 2002. Petrologic case for Eocene slab breakoff during the India–Asian collision. Geology 30, 591–594.

Koulakov, I., Sobolev, S.V., 2006. A tomographic image of Indian lithosphere break-off beneath the Pamir–Hindukush region. Geophys. J. Int. 164, 425–440.

Leech, M.L., Singh, S., Jain, A.K., Klemperer, S.L., Manickavasagam, R.M., 2005. The onset of India–Asia continental collision: early, steep subduction required by the timing of UHP metamorphism in the western Himalaya. Earth Planet. Sci. Lett. 234, 83–97.

Liu, M., Furlong, K., 1993. Crustal shortening and Eocene extension in the southeastern Canadian Cordillera; some thermal and rheological considerations. Tectonics 12, 776–786.

Mattauer, M., 1986. Intracontinental subduction, crust-mantle décollement and crustal-stacking wedge in the Himalayas and other

collision belts. In: Coward, M.P., Ries, A.C. (Eds.), Collision Tectonics. Geol. Soc. Spec. Publ., vol. 19, pp. 37–50.
Minear, J.W., Toksöz, M.N., 1970. Thermal regime of a downgoing slab and new global tectonics. J. Geophys. Res. 75, 1397–1419.
Negredo, A.M., Valera, J.L., Carminati, E., 2004. TEMSPOL: a MATLAB thermal model for deep subduction zones including major phase transformations. Comput. Geosci. 30, 249–258.
Pavlis, G.L., Das, S., 2000. The Pamir–Hindu Kush seismic zone as a strain marker for flow in the upper mantle. Tectonics 19, 103–115.
Pegler, G., Das, S., 1998. An enhanced image of the Pamir–Hindu Kush seismic zone from relocated earthquake hypocenters. Geophys. J. Int. 134, 573–595.
Patriat, Ph., Achache, J., 1984. India–Eurasia collision chronology has implications for crustal shortening and driving mechanisms of plates. Nature 311, 615–621.
Ranalli, G., 1997. Rheology and deep tectonics. Ann. Geofis. 40, 671–680.
Replumaz, A., Tapponnier, P., 2003. Reconstruction of the deformed collision zone between Indian and Asia by backward motion of lithospheric blocks. J. Geophys. Res. 108. doi:10.1029/2001JB000661.
Replumaz, A., Kárason, H., van der Hilst, R.D., Besse, J., Tapponier, P., 2004. 4-D evolution of SE Asia's mantle from geological reconstructions and seismic tomography. Earth Planet. Sci. Lett. 221, 103–113.
Roecker, S.W., 1982. Velocity structure of the Pamir–Hindu Kush region: possible evidence of subducted crust. J. Geophys. Res. 87, 945–959.
Rubie, D.C., Ross, C.R., 1994. Kinetics of the olivine–spinel transformation in subducting lithosphere: experimental constraints and implications for deep slab process. Phys. Earth Planet. Inter. 86, 223–241.
Shimada, M., 1993. Lithosphere strength inferred from fracture strength of rocks at high confining pressures and temperature. Tectonophysics 217, 55–64.
Sibson, R.H., 1981. Controls on low-stress hydro-fracture dilatancy in thrust, wrench and normal fault terrains. Nature 289, 665–667.
Schmeling, H., Monz, R., Rubie, D.C., 1999. The influence of olivine metastability on the dynamics of subduction. Earth Planet. Sci. Lett. 165, 55–66.
Searle, M., Hacker, B.R., Bilham, R., 2001. The Hindu Kush seismic zone as a paradigm for the creation of ultrahigh-pressure diamond- and coesite-bearing continental rocks. J. Geol. 109, 143–153.
Stein, C.A., Stein, S., 1992. A model for the global variation in oceanic depth and heat flow with lithospheric age. Nature 359, 123–129.
Turcotte, D.L., Schubert, G., 2002. Geodynamics, second ed. Cambridge University Press, Cambridge.
Van der Voo, R., Spakman, W., Bijwaard, H., 1999. Tethyan subducted slabs under India. Earth Planet. Sci. Lett. 171, 7–20.
Van Keken, P.E., Kiefer, B., Peacock, S.M., 2002. High-resolution models of subduction zones: implications for mineral dehydration reactions and the transport of water into the deep mantle. Geochem. Geophys. Geosyst. 1056. doi:10.1029/2001GC000256.
Villaseñor, A., Spakman, W., Engdahl, E.R., 2003. Influence of regional travel times in global tomographic models. EGS–AGU–EUG Joint Assembly, Nice.
Vinnik, L.P., Lukk, A.A., Nersesov, I.L., 1977. Nature of the intermediate seismic zone in the mantle of the Pamir–Hindu Kush. Tectonophysics 38, 9–14.